Effect of microstructure on the saturation of swelling in irradiated materials

2001 J. Phys.: Condens. Matter 13 L9

(http://iopscience.iop.org/0953-8984/13/1/102)

INSTITUTE OF PHYSICS PUBLISHING JOURNAL OF PHYSICS: CONDENSED MATTER

J. Phys.: Condens. Matter **13** (2001) L9–L16 www.iop.org/Journals/cm PII: S0953-8984(01)18788-6

LETTER TO THE EDITOR

Effect of microstructure on the saturation of swelling in irradiated materials

S L Dudarev

EURATOM/UKAEA Fusion Association, Culham Science Centre, Abingdon, Oxfordshire OX14 3DB, UK

Received 7 November 2000

Abstract

The interaction of cavities with mobile interstitial clusters is believed to be responsible for the saturation of swelling in irradiated materials. We show that the saturation limit depends on the microstructure of the material, and that the origin of the effect is associated with the violation of the low-density approximation in the case of scattering of one-dimensionally moving interstitial clusters by grain boundaries. For large grains, swelling is enhanced near the boundaries, while for small grains swelling is maximum in the grain interior. The maximum size of cavities corresponding to the saturation of swelling is found to be many times the mean-field estimate.

1. Introduction

Clustering of vacancies and interstitial atoms in collision cascades represents an important element of the kinetics of microstructural evolution of irradiated materials [1–3]. The part played by mobile and immobile interstitial clusters [4], fluctuation effects [5], the anisotropy of diffusion coefficients [6] and the saturation of swelling [7] are among issues that are believed to be fundamentally important for understanding the behaviour of structural materials in the limit of a high irradiation dose [8, 9].

The existing treatment of interactions between mobile interstitial clusters and lattice defects is based on the mean-field approach, where the effective range of motion of clusters in the material is characterized by the mean free path l, where

$$l \sim (N_v a^2)^{-1} \tag{1}$$

in the case of scattering by cavities, and

$$l \sim (\rho d)^{-1} \tag{2}$$

in the case of scattering by dislocation lines [10]. In equation (1) N_v is the volume density of cavities and a is their radius, and in equation (2) ρ is the density of dislocation lines and d is the distance characterizing the effective range of interaction between a mobile interstitial cluster and a dislocation. To describe collisions between mobile and immobile defects in a material using the notion of the mean free path l, we assume that this parameter is many times the average distance between scatterers [11], i.e. $(N_v a^2)^{-1} \gg N_v^{-1/3}$ and $(\rho d)^{-1} \gg \rho^{-1/2}$.

These inequalities are equivalent to the condition that the average density of scattering centres is low $N_v \ll a^{-3}$ and $\rho \ll d^{-2}$.

In the case of scattering of mobile interstitial clusters by grain boundaries the low-density approximation is not satisfied. Indeed, in this case an expression analogous to (1) and (2) has the form

$$l \sim N_{\mathrm{gb}}^{-1} \sim R_g \tag{3}$$

where R_g is the average size of grains, and the condition of validity of the low-density approximation $lN_{\mathrm{gb}} \gg 1$ is violated.

In the case of three-dimensional motion of particles the condition of validity of the low-density approximation is equivalent to the condition that the number of scattering centres in the volume of the order of l^3 is large, and this justifies the mean-field treatment of the problem. The breakdown of the low-density approximation in the case of scattering of one-dimensionally moving clusters by grain boundaries means that considerable deviations from the mean-field picture are likely to occur. The analysis given below confirms this conclusion. In this letter we investigate solutions of equations describing the growth of cavities in an irradiated material. These solutions show that in the presence of grain boundaries the spatial distribution of growing cavities becomes highly inhomogeneous and that the maximum size of cavities corresponding to the saturation of swelling exceeds many times the value calculated using the mean-field approach.

2. The model of growth

Consider a cavity growing in a material irradiated by high-energy neutrons. Point defects and mobile defect clusters formed in collision cascades arrive at the surface of the cavity and make it shrink or grow. The rate of arrival of defects depends on their transport properties, which are radically different for point defects and mobile defect clusters. Single vacancies and interstitial atoms perform three-dimensional diffusional motion in the crystal lattice and their contribution to the rate of variation of the cavity radius $a(\boldsymbol{r}, t)$ is given by [12]

$$\left[\frac{\mathrm{d}a(\boldsymbol{r}, t)}{\mathrm{d}t}\right]_{\text{point defects}} = \frac{1}{a(\boldsymbol{r}, t)}[D_v c_v(\boldsymbol{r}, t) - D_i c_i(\boldsymbol{r}, t)] \tag{4}$$

where D_v and D_i are diffusion coefficients for vacancies and interstitials, and $c_v(\boldsymbol{r}, t)$ and $c_i(\boldsymbol{r}, t)$ are concentrations of point defects. Clusters of interstitial atoms perform one-dimensional diffusional glide [1] and their contribution to the rate of growth is given by

$$\left[\frac{\mathrm{d}a(\boldsymbol{r}, t)}{\mathrm{d}t}\right]_{\text{interst. clusters}} = -\frac{K\epsilon}{4\mathcal{M}} \sum_{k=1}^{\mathcal{M}} \langle \Lambda_k \rangle \tag{5}$$

where $K = G_{\mathrm{NRT}}(1 - \epsilon_r)$ is the effective defect generation rate and ϵ is the cluster formation ratio. Summation over k is performed over directions of one-dimensional motion of clusters in the crystal lattice (i.e. over eight directions of the $\langle 111 \rangle$ type in the bcc lattice and over twelve directions of the $\langle 110 \rangle$ type in the fcc lattice), and $\langle \Lambda_k \rangle$ is the average distance to the nearest scatterer situated on a straight line passing through the centre of the cavity and going in the direction k.

Figure 1 illustrates the derivation of equation (5). The concentration of interstitial atoms performing one-dimensional Brownian motion as a part of a mobile cluster on an interval between two sinks situated at Λ_L and Λ_R equals $C(\Lambda) = (K_c/2D_c)(\Lambda - \Lambda_L)(\Lambda_R - \Lambda)$, where Λ is the coordinate in the direction of the glide and D_c is the effective diffusion coefficient. The flux of interstitial atoms absorbed by the sink situated at Λ_L is equal to

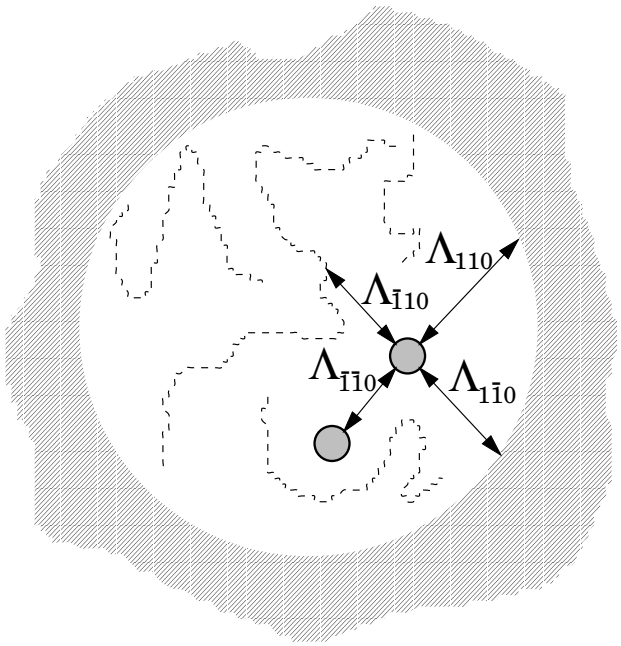

Figure 1. Sketch illustrating the meaning of equation (5). This sketch shows the (001) cross-section of a spherical grain in a fcc crystalline material. In this figure the interstitial clusters moving in the $\langle 110\rangle$ or in the $\langle 1\bar{1}0\rangle$ directions are absorbed by the growing cavity or by the grain boundary. Clusters moving in the $\langle \bar{1}\bar{1}0\rangle$ direction are absorbed by either of the two cavities. Clusters moving in the $\langle \bar{1}10\rangle$ direction are absorbed by either the cavity or by a dislocation.

$J_c = -D_c C'(\Lambda_L) = K_c(\Lambda_R - \Lambda_L)/2$, where $K_c = K\epsilon s_\perp a_0^{-3}\mathcal{M}^{-1}$. In this expression a_0 is the lattice constant and $s_\perp$ is the area of the projection of the Wigner–Seitz cell on the direction of one-dimensional motion. The rate of variation of the number $\mathcal{N}$ of vacancies in a cavity is proportional to the total current of interstitials carried by mobile interstitial clusters

$$\frac{\mathrm{d}\mathcal{N}}{\mathrm{d}t} = -\langle J_c\rangle \frac{\pi a^2(\boldsymbol{r},t)}{s_\perp}. \tag{6}$$

Taking into account that $\mathcal{N}$ is related to the radius of cavity $a(\boldsymbol{r},t)$ via $\mathcal{N}a_0^3 = (4\pi/3)a^3(\boldsymbol{r},t)$, we obtain equation (5).

To find the average distance to the nearest scatterer $\langle\Lambda_k\rangle$ we need to integrate Λ with the nearest-neighbour probability distribution $P_k(\Lambda,\boldsymbol{r})$. This distribution gives the probability of finding a scatterer which is the nearest to a given point $\boldsymbol{r}$ and is situated on a straight line passing through $\boldsymbol{r}$ in the direction defined by the unit vector $\boldsymbol{e}_k$. Function $P_k(\Lambda,\boldsymbol{r})$ satisfies equation [13]

$$P_k(\Lambda,\boldsymbol{r}) = \left(1 - \int_0^\Lambda P_k(\Lambda',\boldsymbol{r})\mathrm{d}\Lambda'\right) n(\boldsymbol{r}+\Lambda\boldsymbol{e}_k) \tag{7}$$

where $n(\boldsymbol{r}+\Lambda\boldsymbol{e}_k)$ is the linear density of scatterers. The solution of (7) is

$$P_k(\Lambda,\boldsymbol{r}) = n(\boldsymbol{r}+\Lambda\boldsymbol{e}_k)\exp\left(-\int_0^\Lambda \mathrm{d}\Lambda' n(\boldsymbol{r}+\Lambda'\boldsymbol{e}_k)\right). \tag{8}$$

In the case of a spatially homogeneous distribution of cavities and dislocations the linear density of scatterers is given by $n = \pi\rho d/4 + \pi N_v a^2$. The average distance $\langle\Lambda\rangle$ to the nearest scatterer in this case is independent of $\boldsymbol{e}_k$

$$\langle\Lambda\rangle = \int_0^\infty \Lambda P(\Lambda, \boldsymbol{r})\mathrm{d}\Lambda = \frac{1}{\frac{\pi}{4}\rho d + \pi N_v a^2}. \tag{9}$$

Substituting this in (4) and (5) we arrive at (see equation (5) in [10])

$$\frac{\mathrm{d}a(t)}{\mathrm{d}t} = \frac{K\epsilon}{a(t)[\rho + 4\pi N_v a(t)]} - \frac{K\epsilon}{\pi\rho d + 4\pi N_v a^2(t)} \tag{10}$$

where it is taken into account that for randomly distributed cavities and dislocations the excess flux of vacancies to the cavity is given by $D_v c_v(t) - D_i c_i(t) = K\epsilon[\rho + 4\pi N_v a(t)]^{-1}$. Solutions of equation (10) satisfying the initial condition $a(0) = a_0 \ll d$ saturate in the limit $t \to \infty$ at $a_{\max} = \pi d$.

3. Analysis of the model

In the case where the motion of a mobile cluster is restricted by the grain boundary, which intersects the line of motion of the cluster at a certain point Λ_g (see figure 2), the nearest-neighbour probability distribution has the form

$$\begin{aligned} P_k(\Lambda, \boldsymbol{r}) &= n(\boldsymbol{r} + \Lambda\boldsymbol{e}_k)\exp\left(-\int_0^\Lambda \mathrm{d}\Lambda' n(\boldsymbol{r} + \Lambda'\boldsymbol{e}_k)\right) \\ &= +\delta(\Lambda - \Lambda_g)\exp\left(-\int_0^{\Lambda_g} \mathrm{d}\Lambda' n(\boldsymbol{r} + \Lambda'\boldsymbol{e}_k)\right). \end{aligned} \tag{11}$$

This probability distribution is defined on the interval $0 \leqslant \Lambda \leqslant \Lambda_g$. The presence of the second term in the right-hand side of equation (11) has a simple meaning: the grain boundary restricts the range of motion of the cluster so that it cannot pass through the boundary into the adjacent grain. Note that equation (11) does not involve calculating averages over the position of the grain boundary. Given condition (3), a calculation of this type would encounter difficulties associated with the summation of a divergent series of terms, see e.g. [14].

In the following we apply (11) to the analysis of the *linear* problem of the growth a cavity in a grain. We assume that the density N_v of cavities satisfies inequality $4\pi^2 N_v d \ll \rho$. In this case dislocations and grain boundaries represent dominant sinks for mobile defects and effects associated with the absorption of mobile defects by other cavities can be neglected. Equation (10) shows that this approximation is not going to influence the limit of saturation of cavity growth, which in accordance with (10) is independent of the volume density of cavities. A similar conclusion also follows from the analysis of the problem of the growth of cavities in the vicinity of a planar grain boundary given in [15].

Consider a spherical grain of radius R_g. The function $\Pi(\boldsymbol{r}) = D_v c_v(\boldsymbol{r}) - D_i c_i(\boldsymbol{r})$, describing the diffusion of point defects, satisfies the equation

$$\frac{1}{r^2}\frac{\mathrm{d}}{\mathrm{d}r}\left(r^2\frac{\mathrm{d}}{\mathrm{d}r}\Pi(r)\right) + K\epsilon - \rho\Pi(r) = 0 \tag{12}$$

the solution of which, subject to the boundary condition $\Pi(R_g) = 0$, is

$$\Pi(r) = \frac{K\epsilon}{\rho}\left[1 - \frac{R_g}{r}\frac{\sinh(\sqrt{\rho}r)}{\sinh(\sqrt{\rho}R_g)}\right]. \tag{13}$$

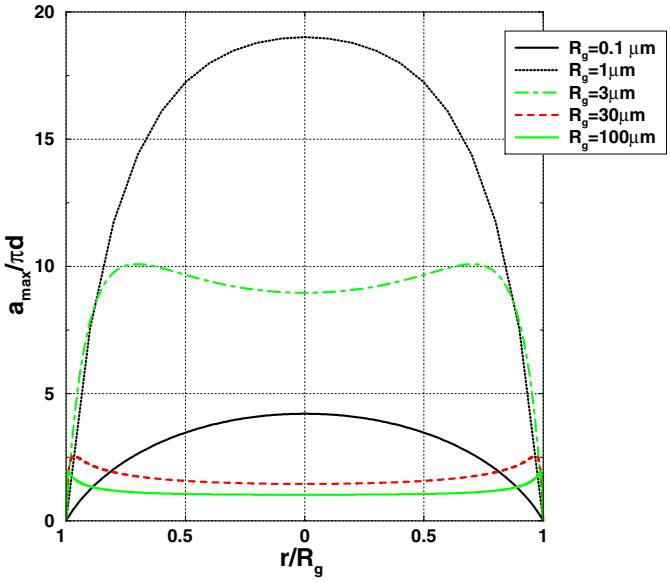

Figure 2. Dependence of the saturation radius $a_{\max}(r)$ on the distance r from the centre of a spherical grain calculated using equation (14) for a bcc ($\mathcal{M} = 8$) crystal. Parameters used in the calculation were $\rho = 10^9$ cm^{-2}, $d = 50$ Å. The coordinates of the cavity $\boldsymbol{r}$ are related to the distance r from the centre of the grain via $\boldsymbol{r} = (r, 0, 0)$.

A straight line passing through the point $\boldsymbol{r}$ in the direction $\boldsymbol{e}_k$, intersects with the grain boundary at points

$$\boldsymbol{r}_{1,2} = \boldsymbol{r} + \boldsymbol{e}_k[(\boldsymbol{r}\cdot\boldsymbol{e}_k) \pm \sqrt{R_g^2 - (\boldsymbol{r}\times\boldsymbol{e}_k)^2}].$$

Substituting this expression in equation (11) and equations (4) and (5), we obtain that the cavity saturation radius depends on the distance r from the centre of the grain and is given by

$$a_{\max}(r) = \pi d \frac{1 - \dfrac{R_g}{r}\dfrac{\sinh(\sqrt{\rho}r)}{\sinh(\sqrt{\rho}R_g)}}{\dfrac{1}{\mathcal{M}}\displaystyle\sum_{k=1}^{\mathcal{M}}\left[1 - \exp\left(-\frac{\pi}{4}\rho d\left|(\boldsymbol{r}\cdot\boldsymbol{e}_k) + \sqrt{R_g^2 - (\boldsymbol{r}\times\boldsymbol{e}_k)^2}\right|\right)\right]}. \quad (14)$$

Figure 2 shows the saturation radius $a_{\max}(r)$ calculated using equation (14) for several values of R_g and plotted as a function of the distance from the centre of the grain. The density of dislocation lines ρ is assumed to remain the same for all the curves shown in figure 2. This figure shows a transition between the case where the diffusion of point defects dominates the kinetics of growth ($R_g \ll (\rho d)^{-1}$), and the case where the shape of the profile is determined by the interaction between cavities and mobile interstitial clusters ($R_g \gg (\rho d)^{-1}$). In the case of small grains the shape of the profile is similar to the one obtained in [16] using the standard rate theory. The similarity between the two cases is not surprising since the kinetic of growth of cavities in small grains is dominated by the diffusion of point defects. In the case of relatively large grains the situation is entirely different. Cavities growing in the interior region of large grains are not affected by processes occurring at grain boundaries, and their saturation radius is equal to the mean-field value πd. Function $a_{\max}(r)$ in the case of large grains is maximum at distance $\sim \rho^{-1/2}$ from grain boundaries, where cavities are able to reach the size $a_{\max} \approx 2\pi d$, which is two times greater than the size corresponding to the saturation of swelling in the grain interior.

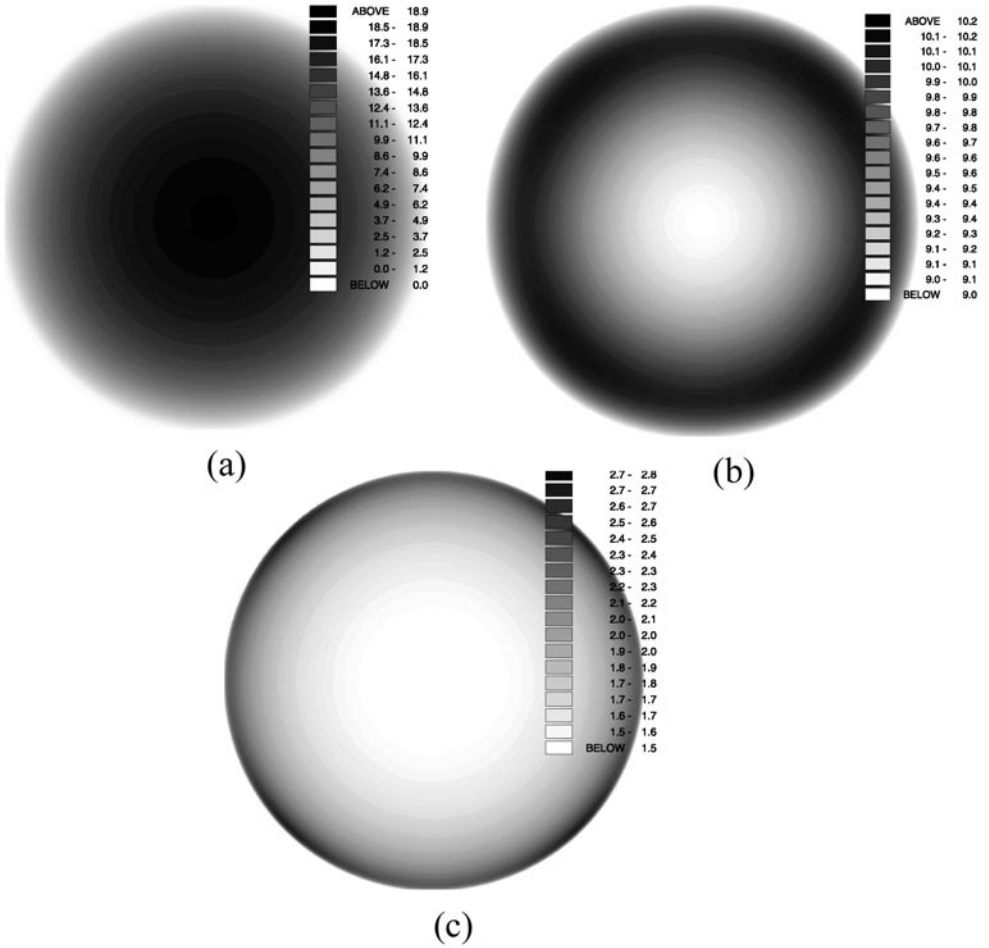

Figure 3. Cross-sections of grains of three different sizes showing the distribution of the saturation radius $a_{\max}(\boldsymbol{r})$ plotted as a function of the position of the cavity in a grain. Each of the three plots shows a cross-section of the grain in the (001) plane. The size of the grain shown in (a) is $R_g = 1$ micron, the size of the grain shown in (b) is $R_g = 3$ micron and the size of the grain shown in (c) is $R_g = 30$ micron. The distributions are plotted in reduced coordinates $(x/R_g, y/R_g)$. Calculations were performed assuming the bcc crystal lattice and $\rho = 10^9$ cm^{-2}.

Figure 3, calculated using equation (14), shows two-dimensional cross-sections of grains of three different sizes illustrating the dependence of the spatial distribution of cavity saturation radii on the size of the grain. For the relatively small grain shown in figure 3(a) the cavity saturation radius is maximum at the centre of the grain. For the large grain (c), cavities reach maximum size (which is this case equals approximately $a_{\max} \approx 2.8\pi d$) in the vicinity of the grain boundary. Figure 3 also shows some relatively weak effects associated with the crystallographic anisotropy of the material. These effects are more strongly pronounced in the case of large grains where the formation of regions of enhanced swelling near grain boundaries is associated with the one-dimensional anisotropic transport of interstitial atoms by mobile clusters.

Probably the most interesting conclusion following the analysis of curves shown in figure 2 and the two-dimensional contour maps shown in figure 3 is that the scattering of mobile clusters by grain boundaries gives rise to a dramatic increase of the limit of saturation of swelling in comparison with the case where cavities grow in the field of randomly distributed dislocations. The fact that scattering by grain boundaries cannot be described by the mean-field approximation results in the formation of regions where profiles of swelling are highly inhomogeneous and where the radius of cavities corresponding to the saturation of swelling by more than an order of magnitude exceeds the maximum size of cavities estimated on the basis of the mean-field approach. For example, for the grain shown in figure 3(b), the maximum size of cavities is approximately 10 times the mean-field value. This corresponds to a 10^3 increase in the swelling saturation limit in comparison with the mean-field estimate. There is no doubt that the topology of grain boundaries (and, in fact, other defects, the segregation of which leads to the formation of planar walls) in a real material is more complex than that of a network of spherical grains considered in the above analysis. However, our analysis shows that the increase of the swelling saturation limit is not associated with a particular choice of the shape of grain boundaries, but rather with the functional form of formula (5). It is the topology of the distribution of extended lattice defects in the material that, in accordance with equation (5), determines the maximum size of cavities. In the case of scattering of mobile interstitial clusters by three-dimensional spherical cavities and two-dimensional dislocation lines, where the mean-field treatment of the problem is fully applicable, swelling saturates at relatively low doses corresponding to the maximum size of growing cavities $a_{\max} \sim d$. In the case of grain boundaries (and dislocation walls) the one-dimensional nature of defect structures leads to the breakdown of the low-density approximation (3) and to the substantial increase of the limit of saturation of swelling. In this case, provided that the growth rates given by equations (4) and (5) do not compensate each other exactly, the rate of swelling is determined by the growth of a relatively small number of 'favourably' positioned cavities, resulting in the linear increase of the total volume of cavities as a function of the irradiation dose.

4. Summary

In this paper we considered effects associated with the violation of the low-density approximation of the statistical theory of scattering in the case of interaction of mobile interstitial clusters with grain boundaries. By analysing the kinetics of growth of cavities using a simple model of a spherical grain we showed that the limit of saturation of swelling is strongly dependent on the topology of the defect structure of the material. This limit may exceed by several orders of magnitude the limit given by the mean-field approximation.

This work was jointly funded by the UK Department of Trade and Industry and by EURATOM. The author is grateful to I Cook for comments. The author wishes to acknowledge stimulating discussions with D J Bacon, Yu N Osetsky, A A Semenov, B N Singh and C H Woo.

References

[1] Bacon D J, Gao F and Osetsky Yu N 2000 *J. Nucl. Mater.* **276** 1
[2] Woo C H 1999 *J. Comp. Aided Mater. Design* **6** 247
[3] Singh B N 1999 *Radiat. Effects Defects Solids* **148** 383
[4] Singh B N, Golubov S I, Trinkaus H, Serra A, Osetsky Yu N and Barashev A V 1997 *J. Nucl. Mater.* **251** 107
[5] Semenov A A and Woo C H 1998 *Appl. Phys.* A **67** 193
[6] Borodin V A 1998 *Physica* A **260** 467
[7] Golubov S I, Singh B N and Trinkaus H 2000 *J. Nucl. Mater.* **276** 78

[8] Matthews J R 1977 *Contemp. Phys.* **18** 571
[9] Eyre B L and Matthews J R 1993 *J. Nucl. Mater.* **205** 1
[10] Trinkaus H, Singh B N and Foreman A J E 1992 *J. Nucl. Mater.* **199** 1
[11] Ziman J M 1979 *Models of Disorder* (Cambridge: Cambridge University Press) section 13
[12] Brailsford A D and Bullough R 1972 *J. Nucl. Mater.* **44** 121
[13] Chandrasekhar S 1943 *Rev. Mod. Phys.* **15** 1
[14] Doniach S and Sondheimer E H 1998 *Green's Functions for Solid State Physicists* (London: Imperial College Press) section 5 pp 96–109
[15] Dudarev S L 2000 *Phys. Rev.* B **62** 9325
[16] Singh B N and Foreman A J E 1974 *Phil. Mag.* **29** 847